Initial Embedding of Functional Sensors in Additively Manufactured Silicon Carbide

Adrian M. Schrell[*,†], Dylan Richardson[*], Brian C. Jolly[*], Kurt A. Terrani[*], and Christian M. Petrie[*]

[*] *Oak Ridge National Laboratory, 1 Bethel Valley Road, Oak Ridge, TN 37831*
[†] *schrellam@ornl.gov*

https://dx.doi.org/10.13182/T123-33579

INTRODUCTION

For new nuclear plants to be cost competitive with natural gas and renewable energy sources, the plants must be able to continually deploy new technologies and adapt the size and cost of new reactors to changing market conditions. To this end, the Department of Energy's Office of Nuclear Energy has funded the Transformational Challenge Reactor (TCR) program. TCR aims to combine advanced manufacturing, in situ process monitoring, and data analytics to rapidly design, build, and test an advanced nuclear reactor [1]. Additive manufacturing technologies can be used to rapidly build and deploy new reactor concepts and technologies that are not subjected to the same constraints associated with traditional manufacturing. These same technologies are being used to introduce high performance materials into these systems. Integrating online process monitoring could accelerate qualification and deployment of critical components. Finally, additive manufacturing processes are well suited for direct embedding of sensors inside reactor components at strategic locations for online monitoring of reactor health and operating parameters.

Embedded sensors allow for real time measurements of parameters such as temperature, strain, or neutron flux at critical locations that may not be accessible after component fabrication is complete. Because TCR is utilizing additive manufacturing to build the reactor core, sensors can be inserted at a desired location as the components are fabricated. The TCR core is composed primarily of SiC ceramic material [2]. SiC is attractive due to its tolerance to neutron irradiation, high temperatures, and exposure to a wide range of chemical environments [3]. Therefore, the sensors must be compatible with the SiC ceramic additive manufacturing process.

Fiber-optic sensors are being considered for embedding in SiC ceramics because they can provide spatially distributed measurements of strain and temperature measurements in real time. Fiber optics have been demonstrated to withstand high temperatures [4-6] as well as moderate irradiation dose [7-10]. Additionally, the difference in the coefficient of thermal expansion (CTE) between amorphous fused silica (SiO_2) and SiC could allow the fiber-optic sensors to survive higher temperatures compared with those embedded in metals [11, 12], which have a much higher CTE. This work describes the first attempt to embed functional sensors in a 3D-printed SiC [13] component and the lessons learned that will inform future testing.

EXPERIMENTAL APPROACH

The additive manufacturing process that is being used to produce 3D-printed SiC parts for the TCR first uses binder jet 3D printing technologies to print intricate parts out of SiC powder held together by an organic binder. Chemical vapor infiltration (CVI) is then used to drive off the binder and densify the parts. This process uses methyltrichlorosilane (MTS) to penetrate into the porous SiC component where it thermally decomposes to form solid SiC. CVI of SiC components is typically performed at temperatures in the range of ~1000 °C over the course of a few days. The initial temperature increase drives off the organic binder, and the MTS decomposes into SiC and HCl gas to slowly densify the part to ~90% of theoretical density [13]. The combination of high temperatures and a harsh chemical (HCl) environment presents challenges for choosing materials and sensors that can survive the CVI process. Thermodynamic calculations and material compatibility tests have shown that SiO_2 optical fibers and various refractory metals are capable of surviving the CVI process [14]. Fiber-optic sensors are being considered for both strain (directly embedded into SiC) and temperature (loose fibers inside an embedded metal sheath) monitoring.

To embed metal sensor sheathes, the SiC parts are 3D printed with a hole similar in size to the sheath. Then the sheath, which is a closed-ended tube, is press-fit into the part. Once the sheath is inserted, the CVI process densifies the part and deposits SiC at the sheath/SiC interface, thus embedding the sheath in the SiC component. For direct embedding of optical fibers into SiC parts, the parts are printed with an oversized channel or cavity. Next, optical fibers are inserted into the cavity, filled with loose SiC powder, and vibrated to allow the powder to settle. In most cases, an open-ended refractory metal sheath is placed over the optical fiber lead and is partially inserted into the packed SiC powder. This sheath provides mechanical protection of the fiber as it passes out of the CVI system.

RESULTS AND DISCUSSION

Figure 1 shows a picture of a 3D-printed SiC can with two fiber-optic sensors that were directly embedded in the can. Each sensor has a molybdenum sheath that is partially embedded in the can. The outer shell of the can was printed using the binder jet process as described earlier. The inside of the can was filled with loose SiC powder and densified using CVI. After CVI, one of the two fibers could be observed passing out of its sheath. The other could not be observed and likely broke somewhere inside of the sheath.

X-ray computed tomography (XCT) was performed on the entire assembly after CVI to provide more detail on the internal features of the can with embedded sensors. Figure 2 shows transverse cross-sectional images of the can with embedded sensors in two different planes. The molybdenum sheath that contained the accessible optical fiber lead was easily removed from the printed can, indicating that it was not strongly bonded to the SiC matrix. The fiber contained inside that sheath was also removed easily, and it appeared that this fiber broke near the start of the embedded region.The other sheath did appear to be well bonded, at least over a portion of its length, based on the XCT images and the fact that it could not be easily removed. The low-density SiO_2 fiber-optic sensors are difficult to see in the images but are more clearly visible in the region of the SiC matrix in which the sensors are embedded.

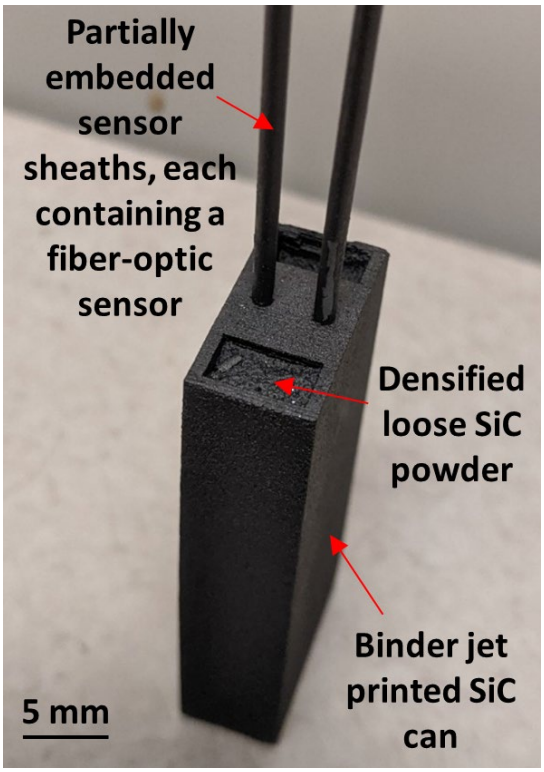

Fig. 1. Picture of printed SiC can with embedded, sheathed fiber-optic sensors.

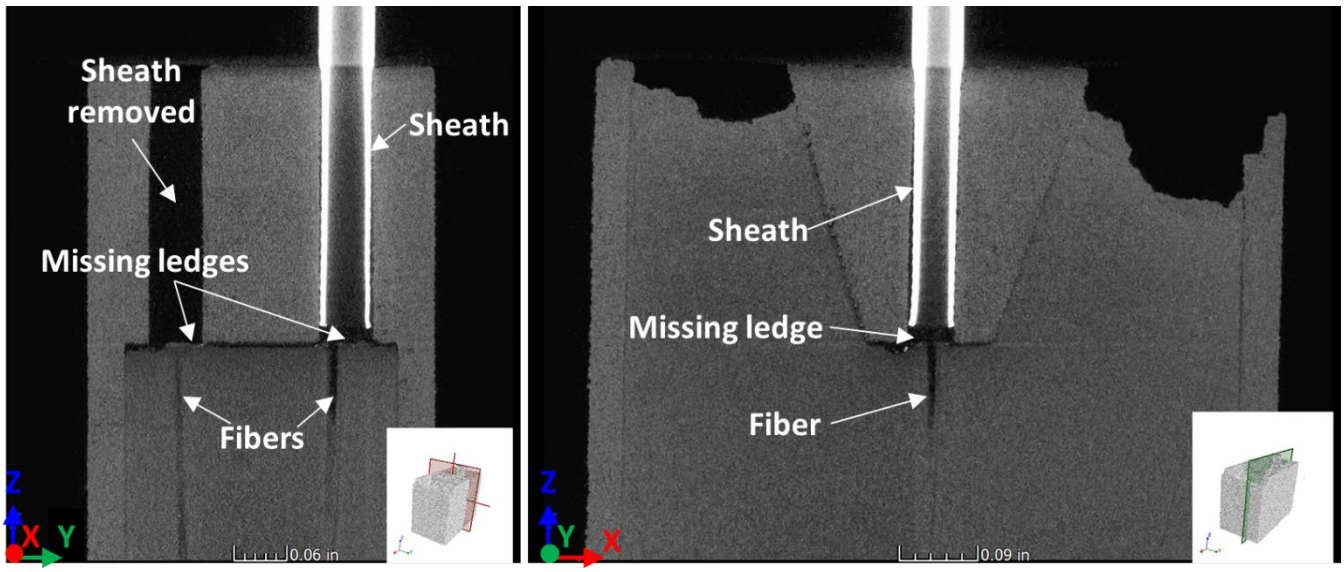

Fig. 2. Transverse cross-sectional images in two different planes obtained from XCT of a printed SiC can with embedded, molybdenum-sheathed fiber-optic sensors.

The XCT images provide additional information that will inform future sensor embedding trials. First, the sensor cans were printed with ledges above the embedded fiber region (Fig. 2). The intent was to have the sheaths rest on these ledges before the loose powder is poured into the can. Because these ledges do not appear in the post-CVI XCT images, it appears that those ledges were broken during either loading or CVI. It is possible that when the ledge broke the dense molybdenum sheath fell down on top of the fragile optical fibers, causing the fibers to break where they exit the

embedded region. Future tests will use a thicker ledge to hopefully prevent the ledge from breaking. Another interesting observation from the XCT images is that one of the fibers shown in the YZ plane is not concentric with its sheath. It appears that this fiber is close to contacting one side of the sheath's inner surface. This concentricity issue could make the fiber more susceptible to breaking if the sheath were to move at all during CVI. In addition, it is possible that the fiber could bond to the inner surface of the sheath as SiC material is deposited during CVI. This concentricity will be considered when modifying the can design for future tests. Both issues (the lack of a ledge and the concentricity of the fiber and its sheath) would not be a concern when embedding loose fibers inside of a closed-ended metal sheath (i.e., for temperature sensing).

CONCLUSIONS

This work summarizes the initial attempts to embed functional fiber-optic sensors in 3D-printed SiC parts in support of the TCR. Silica optical fibers have been successfully embedded in SiC, with the ultimate goal of spatially distributed strain and temperature monitoring. However, XCT of the embedded sensors showed that there are still additional issues to overcome to ensure that the fibers leads are not broken either during handling or the densification of the SiC matrix during CVI. Those issues include (1) the design of small features in the SiC can that appeared to fracture during CVI and (2) the concentricity of the fiber-optic sensors with their metal sheaths.

ACKNOWLEDGMENTS

This research is sponsored by the TCR program of the US Department of Energy, Office of Nuclear Energy.

REFERENCES

1. ORNL. *Transformational Challenge Reactor: Demonstrating a faster, more affordable approach to advanced nuclear energy*. [cited 2020 1-26-2020]; Available from: tcr.ornl.gov.
2. B.R. BETZLER, et al., "Transformational Challenge Reactor Preconceptual Core Design Studies," *Nuclear Engineering and Design* (Accepted).
3. T. BYUN, et al., "Mechanical and Thermophysical Properties of 3D-Printed SiC - FY 2020," ORNL/SPR-2020/1545, Oak Ridge National Laboratory (2020).
4. T.W. WOOD, et al., "Evaluation of the Performance of Distributed Temperature Measurements with Single-Mode Fiber Using Rayleigh Backscatter up to 1000°C," *IEEE Sensors Journal* **14**, 124-128 (2014).
5. B.A. WILSON, C.M. PETRIE, and T.E. BLUE, "High-temperature effects on the light transmission through sapphire optical fiber," *Journal of the American Ceramic Society* **101**, 3452-3459 (2018).
6. C.M. PETRIE and T.E. BLUE, "In Situ Thermally Induced Attenuation in Sapphire Optical Fibers Heated to 1400°C," *Journal of the American Ceramic Society* **98**, 483-489 (2015).
7. C.M. PETRIE, A. BIRRI, and T.E. BLUE, "High-dose temperature-dependent neutron irradiation effects on the optical transmission and dimensional stability of amorphous fused silica," *Journal of Non-Crystalline Solids* **525**, 119668 (2019).
8. C.M. PETRIE, et al., "Reactor radiation-induced attenuation in fused silica optical fibers heated up to 1000 °C," *Journal of Non-Crystalline Solids* **409**, 88–94 (2015).
9. C.M. PETRIE and T.E. BLUE, "In situ reactor radiation-induced attenuation in sapphire optical fibers heated up to 1000 °C," *Nuclear Instruments and Methods in Physics Research Section B: Beam Interactions with Materials and Atoms* **342**, 91–97 (2015).
10. C.M. PETRIE, B. WILSON, and T.E. BLUE, "In Situ Gamma Radiation-Induced Attenuation in Sapphire Optical Fibers Heated to 1000°C," *Journal of the American Ceramic Society* **97**, 3150-3156 (2014).
11. C.M. PETRIE, et al., "Embedded metallized optical fibers for high temperature applications," *Smart Materials and Structures* **28**, 055012 (2019).
12. C.M. PETRIE, et al., "High-temperature strain monitoring of stainless steel using fiber optics embedded in ultrasonically consolidated nickel layers," *Smart Materials and Structures* **28**, 085041 (2019).
13. K. TERRANI, B. JOLLY, and M. TRAMMELL, "3D printing of high-purity silicon carbide," *Journal of the American Ceramic Society* **103**, 1575-1581 (2020).
14. C.M. PETRIE, et al., "Embedment of sensors in ceramic structures," ORNL/SPR-2019/1301, Oak Ridge National Laboratory (2019).